PROCEEDINGS OF SPIE

SPIEDigitalLibrary.org/conference-proceedings-of-spie

Incorporating structural analysis in a quantum dot Monte-Carlo model

I. M. E. Butler, Wei Li, S. A. Sobhani, N. Babazadeh, I. M. Ross, et al.

I. M. E. Butler, Wei Li, S. A. Sobhani, N. Babazadeh, I. M. Ross, K. Nishi, K. Takemasa, M. Sugawara, Negin Peyvast, D. T. D. Childs, R. A Hogg, "Incorporating structural analysis in a quantum dot Monte-Carlo model," Proc. SPIE 10553, Novel In-Plane Semiconductor Lasers XVII, 105530G (19 February 2018); doi: 10.1117/12.2291004

SPIE.

Event: SPIE OPTO, 2018, San Francisco, California, United States

Incorporating structural analysis in a quantum dot Monte-Carlo model

I.M.E. Butler*[1,2], Wei Li[3], S.A. Sobhani[1], N. Babazadeh[1], I.M. Ross[3], K. Nishi[4], K. Takemasa[4], M. Sugawara[4], Negin Peyvast†[3], D.T.D. Childs[1], and R.A. Hogg[1]

[1] School of Engineering, University of Glasgow, Glasgow, G12 8LT, UK
[2] School of Mathematics and Physics, Queens University Belfast, Belfast, BT7 1NN, UK
[3] Department of Electronic & Electrical Engineering, University of Sheffield, Sheffield, S1 4DE, UK
[4] QD Laser Inc, Keihin Bldg. 1F, 1-1 Minamiwataridacho, Kawasaki-ku, Kawasaki, Kanagawa 210-0855, JAPAN

ABSTRACT

We simulate the shape of the density of states (DoS) of the quantum dot (QD) ensemble based upon size information provided by high angle annular dark field scanning transmission electron microscopy (HAADF STEM). We discuss how the capability to determined the QD DoS from micro-structural data allows a Monte-Carlo model to be developed to accurately describe the QD gain and spontaneous emission spectra. The QD DoS shape is then studied, with recommendations made via the effect of removing, and enhancing this size inhomogeneity on various QD based devices is explored.

Keywords: Quantum Dots, HAADF STEM, inhomogeneous broadening

1. INTRODUCTION

Self-assembled quantum dot (QD) lasers are a commercially viable option in a range of devices from sensing through to communication systems.[1–3] Improvement in modulation bandwidth has seen vast advancements due to new epitaxial processes. They have been an active research area for several decades and been of interest due to their low threshold current and temperature insensitivity[4] due to their delta-like density of states (DoS). The control of inhomogeneous broadening has been vital in improving the QD offering.

While these developments can be studied and monitored via optical spectroscopy, limited information is known about the micro-structure of the QD ensemble after the capping of GaAs. Feedback between epitaxial processes, size and compositional variation and shape of the DoS important. In this paper we address this need, linking real parameters of the QD ensemble in QD modelling, where a new route to model QDs is described with measured TEM. The shape of the DoS is then discussed and examined to provide recommendations based on altering the ensemble size range.

2. DEVICE STRUCTURE

The device measured is as follows. The epitaxial structure of the QD material was grown using molecular beam epitaxy (MBE). Using a GaAs substrate, QDs are grown on the (100) plane, the QD active layer structure is made up of a InAs QD layer for Stranski-Krastanov (S-K) growth, a InGaAs strain reducing layer[5,6] capped by a GaAs capping layer. The active region is sandwiched between n- and p-doped AlGaAs cladding layers, to provide optical confinement and electrical injection. Growth parameters have been discussed extensively elsewhere[5,7,8]

* Send correspondence to Iain.Butler@glasgow.ac.uk
† Now with Oclaro UK, Towcester, Northamptonshire, NN12 8EQ, United Kingdom

Novel In-Plane Semiconductor Lasers XVII, edited by Alexey A. Belyanin, Peter M. Smowton, Proc. of SPIE Vol. 10553, 105530G · © 2018 SPIE · CCC code: 0277-786X/18/$18 · doi: 10.1117/12.2291004

3. INITIAL MODEL

There are various methods of modelling and simulating QD gain/spontaneous emission (SE). An example of this is the full quantum treatment approach,[9] which applies carrier-carrier and carrier-phonons effects. While this approach provides thorough calculation of free-carrier effects, it has been noted that finding the exact parameters which will simulate experimental results remains difficult to produce a match.[10–12] Another model developed,[13] is described in figure 1 showing our starting approach. The unique feature of this model is that it utilises both empirical and measured input parameters, which is seen after the indium clustering process during Stranski-Krastanov growth.[14] Input parameters such as state separation and inhomogeneous broadening can be captured via spectroscopic methods such as photoluminescence (PL), low current density electroluminescence (EL) and photocurrent (PC). Assuming the inhomogeneous distribution is Gaussian, a full width half maximum (FWHM) can be used for ensemble inhomogeneity. While inhomogeneous and homogeneous broadening will be convoluted together however homogeneous broadening provides smaller broadening than inhomogeneous.[15]

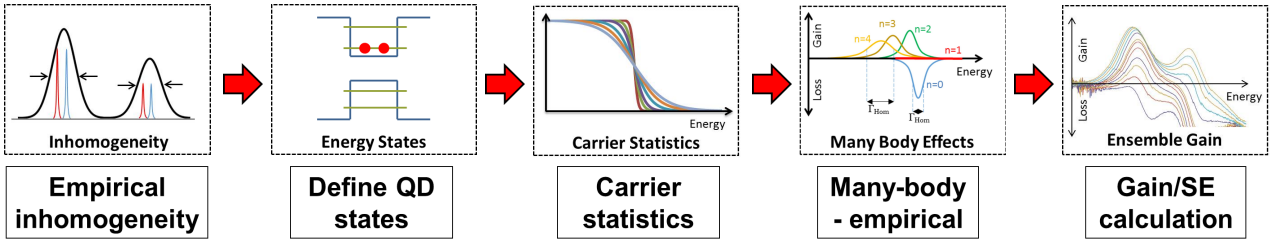

Figure 1. Modelling quantum dot gain and spontaneous emission approach from[13] .

State separation is defined experimentally to be constant across the ensemble. QD states are defined from the carrier thermal energy using the state separation. Carrier statistics can be chosen via a fermi distribution or a random distribution.[16] Carrier relaxation times are neglected and simulated as instantaneous, creating a distribution of instantaneous occupancy across the ensemble.

Once the ensemble (typically 10^6 quantum dots) has been filled, many-body effects maybe applied. Figure 1 step 4 shows how systematically the gain is calculated for each QD. While the SE component will be most energetic and narrow where the QDs are of equal size (where inhomogeneous broadening = 0), increasing this broadening causes the total energy decreases and increases linewidth. The assumption is made that each QD will have a constant recombination lifetime and oscillation strength. Further normalisation and inhomogeneous broadening is added to each QD gain/SE spectra based on the occupancy of the given QD. Importantly when there is 0 carriers for the given QD absorption occurs, leading rise to a reliable simulation.

Figure 2 compared the gain spectrum as a result of this model with a comparison to measured gain spectrum. Gain was calculated using the well-known Hakki-Paoli method.[17] Inhomogeneous broadening fixed at 42meV, state separation of 85meV and a homogeneous broadening of 5meV. Figure 2 (a), shows a comparison at 2 different current (average carrier) densities, dark colour (online colour) corresponds to 0.5kAcm^{-2} (2.7) and the blue colour 2.7kAcm^{-2} (6.3). The peak red-shifts from 0.97eV to 0.96eV, there is also a 30% increase in gain. Increasing the carrier density (and thus current density), the peak red-shifts further and gain increases until gain saturation G_{sat} is achieved. However we have found that the fit of the ES peak and GS-ES ratio at low current densities at high energy to be disappointing over the whole spectral range.

4. ROUTE TO NEW MODEL

Using the previous model as a starting point, if the micro-structure of the QD ensemble is known (via measurement). This would provide a new route to simulate QD ensembles, allowing the quantum structures to use real size information. Figure 3 shows this potential change to the model, noting that measure structure and calculated the QD states have now replaced the empirical inhomogeneity and defined QD states.

The structure can be measured via atomic force microscopy (AFM) or transmission electron microscopy (TEM), the individual QD size/diameter can be measured due to either the surface topology or changes in

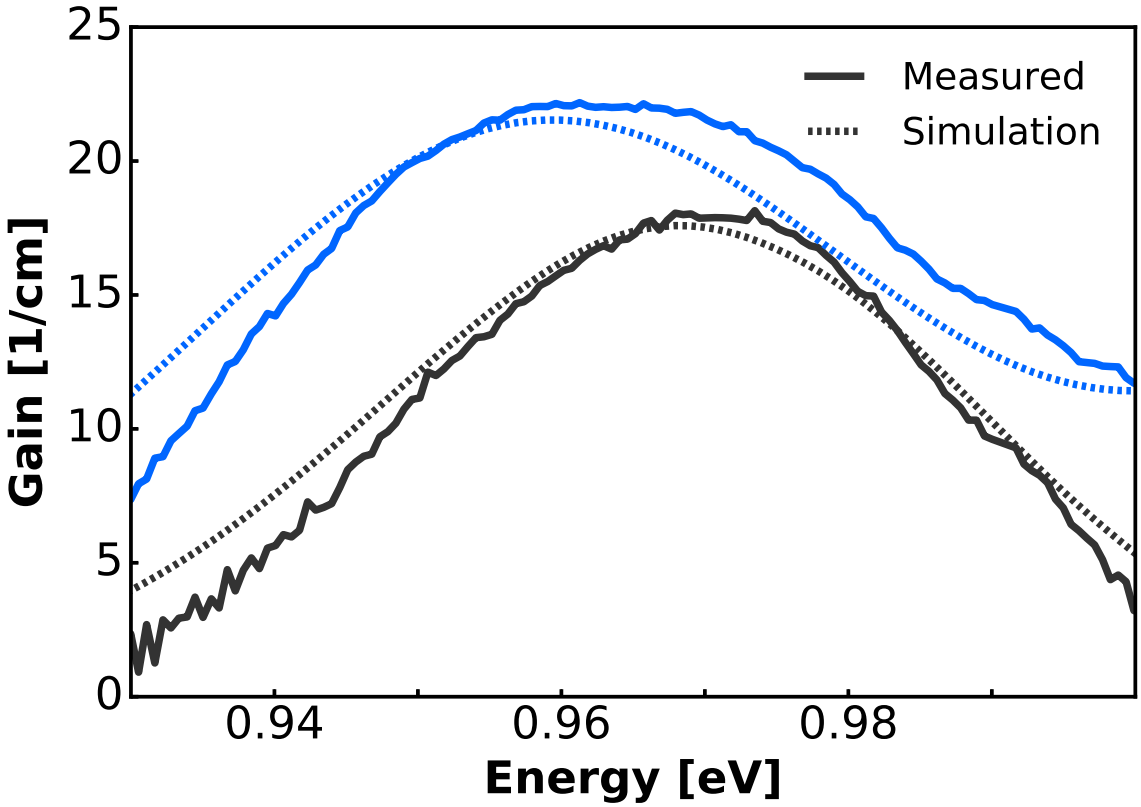

Figure 2. Gain results from model described in section 3. Measured gain is calculated using the Hakki-Paoli method.[17] a) Shows a comparison at current densities (average carrier); dark colour = 0.5kAcm^{-2} (2.7) and blue = 2.7kAcm^{-2} (6.3).

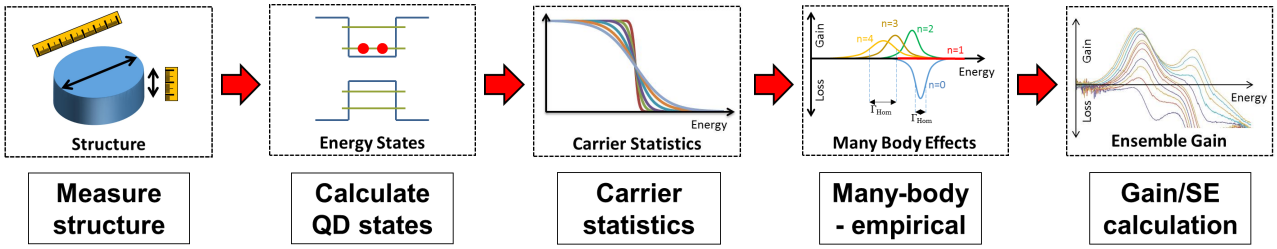

Figure 3. Modelling quantum dot gain and spontaneous emission using an new approach inspired by[13] .

material composition. Previously to measure the micro-structure uncapped QDs were measured using ARM,[18] however reports in literature suggested that QD shape maybe affected when capped.[19,20] A cross-section of the active region can be examined using TEM, which will enables buried structural information to be seen.

Using the measured sizes/diameters would then allow the QD states to be calculated, the initial model can be adapted to accept these states. Resulting in gain and SE calculated from known QD micro-structure.

4.1 Transmission Electron Microscopy - Structural Measurement

To measure the structure of the QD ensemble within the epitaxial layers, high angle annular dark field scanning transmission electron microscopy (HAADF STEM) enables the compositional information to be retrieved. HAADF intensity is very sensitive to Z (atomic number) and is approximately proportional to the square of Z, which will result in changes of contrast in the QD due to indium composition. Due to the difference in Z, indium will appear brighter, relative to gallium which will cause the QD to be highlighted, from the GaAs capping layer.

Figure 4 (a) shows an example of HAADF STEM imaging for a single QD, within one of the QD active region layers. The lighter contrast region shows the single QD. The region around the QD is the capping layer of GaAs and the area below the QD is of the wetting layer and SRL.[21] Images were acquired with a JEOL R005 aberration corrected TEM/STEM operating at 300kV with a convergence semi-angle of 21mrads and a STEM inner annular collection angle of 62mrads. Cross-sectional STEM samples were prepared by argon ion milling at an acceleration voltage of 3kV and incident angle between 6°and 12°until hole perforation was achieved.

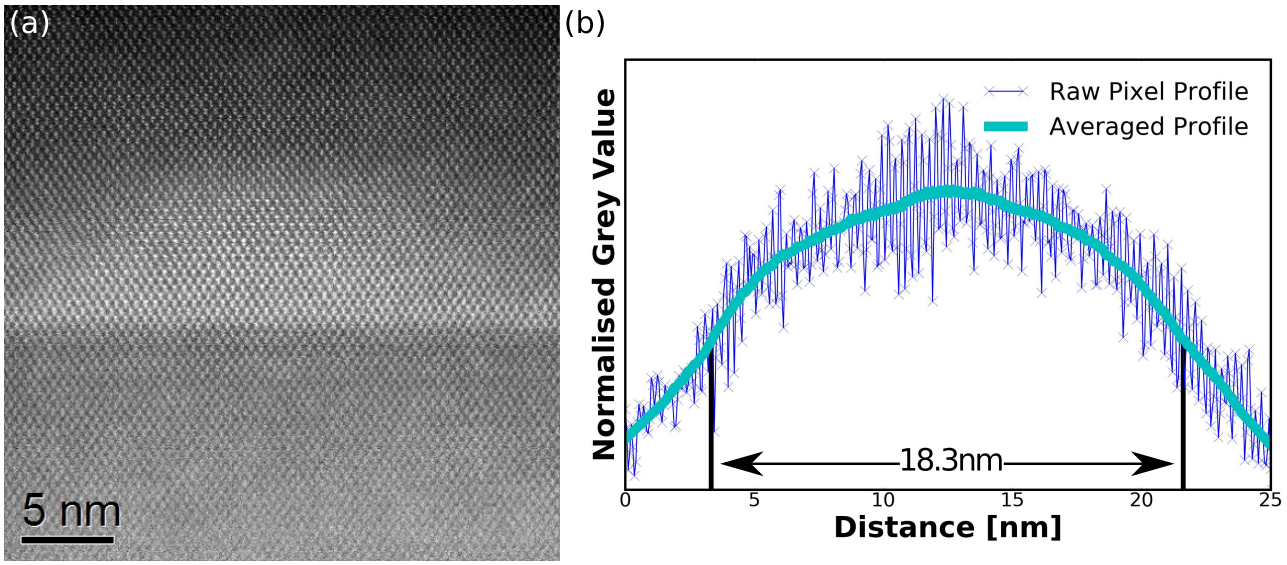

Figure 4. a) HAADF STEM image of a QD. b) Pixel (vertically integrated) profile of QD pictured. Raw pixel profile plot and averaged profile to take FWHM.

By adjusting scales with the scale bar, size information for the given QD can be achieved. A pixel intensity profile can be taken as shown in figure 4 (b). The pixel profile which is vertically integrated to minimize noise caused by the hole perforation. The shape is a typical distribution of indium over the QD.[22] FWHM is found to be 18.3nm, assuming that the QD is of equal diameter confinement energy can be calculated as follows.

4.2 Calculate QD Energy States

$$E_{emission} = E_{gap} + \frac{\hbar^2\pi^2}{2m_e^*}\left[\left(\frac{n_x}{L_x}\right)^2 + \left(\frac{n_y}{L_y}\right)^2 + \left(\frac{n_z}{L_z}\right)^2\right] + \frac{\hbar^2\pi^2}{2m_h^*}\left[\left(\frac{n_x}{L_x}\right)^2 + \left(\frac{n_y}{L_y}\right)^2 + \left(\frac{n_z}{L_z}\right)^2\right] \quad (1)$$

To calculate the QD states, we use a 3d solution to Schrödingers time-independent equation assuming infinite potential barriers as shown in equation 1. Where E_{gap} = material band gap, m_e^* = electron effective mass, m_h^*

= hole effective mass, n_x = quantum energy level number in x direction, n_y = quantum energy level number in y direction, n_z = quantum energy level number in z direction, L_x = width of potential well in x direction, L_y = width of potential well in y direction, L_z = width of potential well in z direction and all other mathematical constants reflect their natural value.

The assumption of a circular QD causes $L_x = L_y$, the height is fixed at 7nm.[23] The material band gap is calculated using a linear interpolation with a bowing parameter.[24] Effective mass is calculated based on the indium concentration as a linear interpolation between the binaries of InAs and GaAs.

The ability to input a range of sizes, allows a distribution to be created which can be useful if the QD ensemble as a range of QD sizes/shapes. The model uses a chance matrix to intermix confinement energies permutations to create an energy distribution of the input likelihood of a QD with the given size and number.

4.3 Transition Energy and Indium Composition

Figure 5 shows the effect of indium composition on 3 QD sizes (height is kept constant at 7nm) assuming the indium concentration is equal across the whole QD. Transition energy versus the indium composition with a comparison of different dot diameters. The lowest transition energy for a given QD is attributed to the transition of the first electron level to the first heavy hole level. This transition is known as the ground state (GS). Likewise the next lowest confinement, is related to the transition between the 2nd allowed electron and heavy hole level or the first excited state (ES). Noting that no sub bands are accounted for in this model. Increasing the dot size causes a close to parallel decrease in energy. A good agreement is shown between GS, ES and state separation

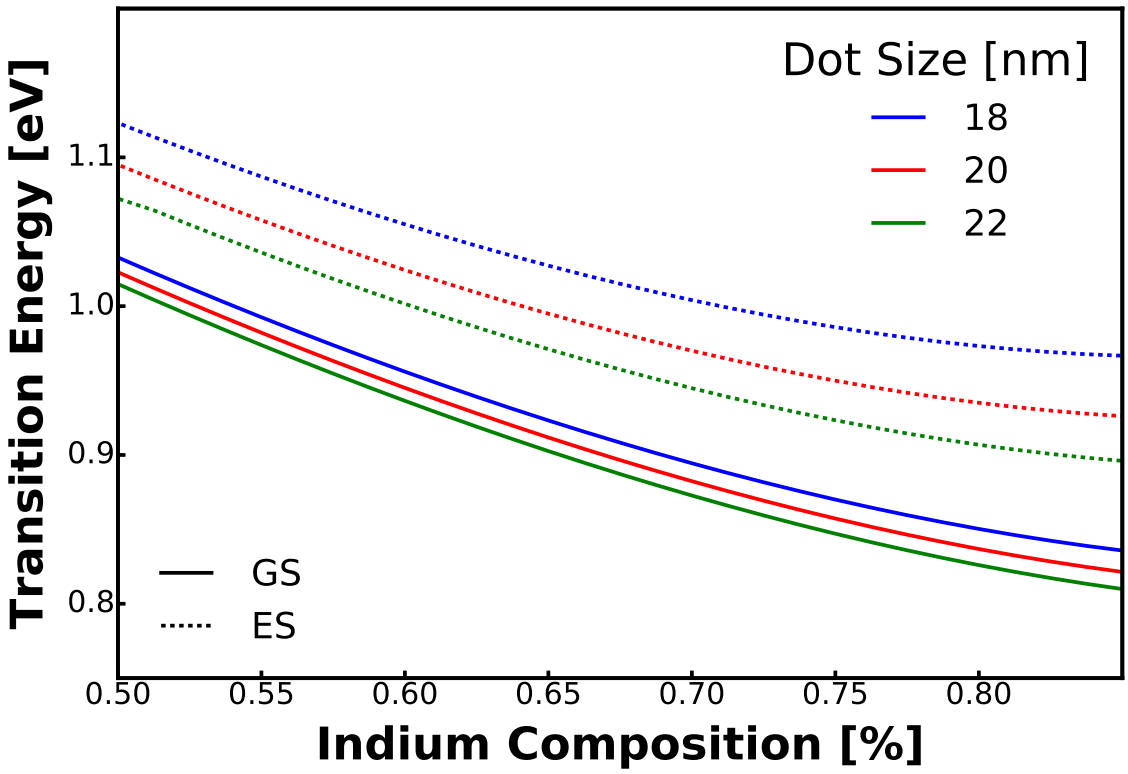

Figure 5. A comparison, of confinement energy with a variation of indium composition and quantum dot size. Ground state shown as solid line and excited state as dotted, colour (online) with respect to dot size.

(ΔE) to previously reported results.[25,26] While assumptions are made in this model, it shows that the simple model is able match measured state separation.

4.4 Density of States Shape

A graphical view of the QD quantum states is built by modelling the shape of density of states. This analysis will show the GS and ES, with the range of allowed energies that carriers will be able to occupy. The DoS shape is visualised by summing the calculated confinement energies into equal energy bins. Narrow and well defined peaks would be expected at the DoS for a narrow linewidth laser

Figure 6 shows 3 separate graphs of how changing the input QD size distribution affects the distribution of transition energies. Result A, uses a single QD of diameter 18.3nm as measured from fig. 4 and an indium concentration of 60%. Resulting in a narrow single peak at 0.988eV and 1.083eV, showing the location of the GS and ES. As expected the ES has double the degeneracy of the GS.

Result B, added further complexity and utilising the freedom of inputting exact sizes of QDs and the likelihood. 4 QDs of equal chance are used with a diameter of 18nm, 18.3nm, 18.6nm & 19nm (0.25 chance of each size). Small variation has cause the GS and ES to broaden. A red-shift is observed with the GS (ES) peak at 0.987eV (1.078eV). The height of the DoS has decreased, where the integral of components is equal to the single QD result (shown in A).

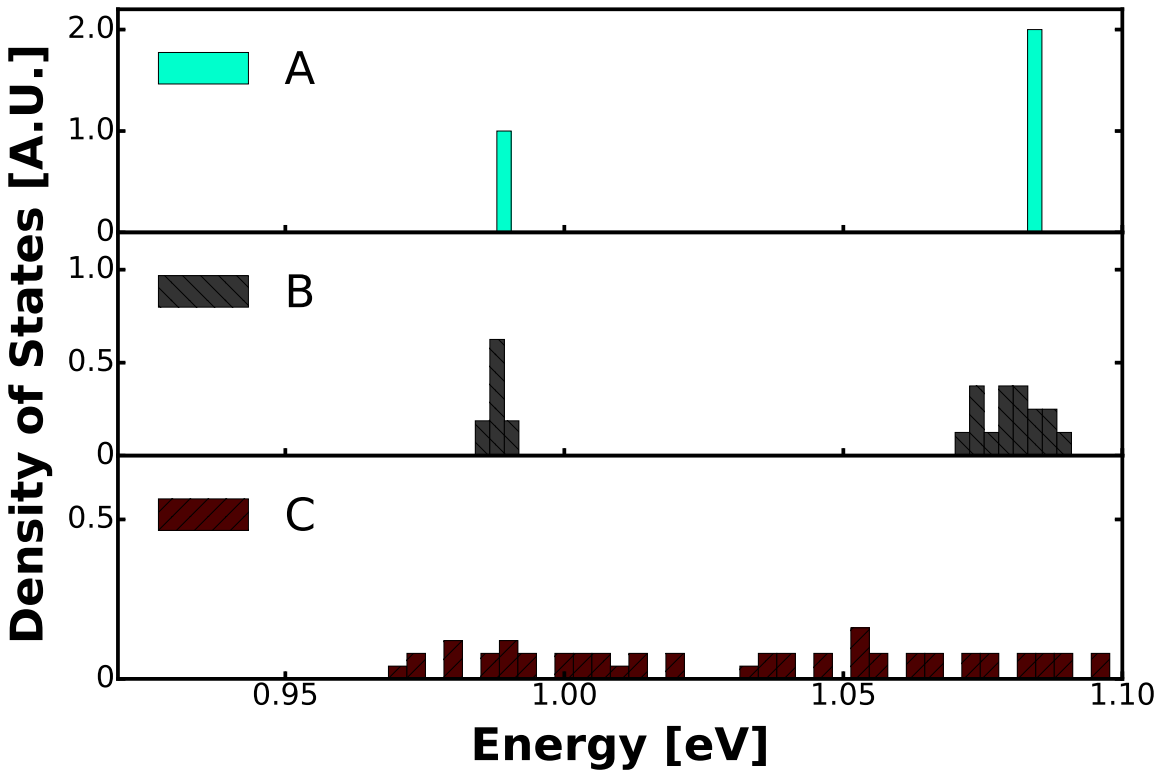

Figure 6. Comparison of different QD distributions with increasing inhomogeneity. A) models the HAADF STEM QD from fig. 4 (a single QD with a width of 18.3nm in all directions. B) A range of QDs with 4 different widths in the orthogonal planes all with equal chance. Variation of 18.5 ±0.5nm. C) Further inhomogeneity series of 5 widths ranging from 14nm - 22nm.

Result C, explores how this inhomogeneity fosters itself and affects the DoS shape. 5 QDs of equal chance are used with a range of 14nm - 22nm (step 2nm). The GS and ES have become very broad and difficult to predict the peak energy.

The results from figure 6 show that inhomogeneous broadening has large affect on the DoS. Noticeably the improvement from B towards A, is the thrust of epitaxial processes.[5,27] An improvement of the GS and ES line-width at the DoS is likely to provide an enhancement of laser performance. Interestingly, the broadening of GS and ES, B towards C creates an opportunity for broad spectral bandwidth applications.[28]

5. CONCLUSION

In summary, we have described and presented a new route to model QD gain and SE. Allowing for the shape and distribution to be measured from a real structure. Methods of measuring QDs have been discussed and a model to calculate the QD energy states with the DoS shape has been introduced. This model has shown that increasing the inhomogeneity adversely affects the shape and distribution of the DoS. Future work will concentrate on carefully linking the optical-electric properties of QDs with observed micro-structure.

ACKNOWLEDGMENTS

This work was supported by the Engineering and Physical Sciences Research Council (RCUK Grant No. EP/L015323/1).

REFERENCES

[1] Akiyama, T., Sugawara, M., and Arakawa, Y., "Quantum-dot semiconductor optical amplifiers and laser diodes for optical communications," (sep 2007).

[2] Tanaka, Y., Takada, K., Ishida, M., Nakata, Y., Yamamoto, T., Yamaguchi, M., Nishi, K., Sugawara, M., and Arakawa, Y., "High-speed modulation in 1.3-m inas/gaas high-density quantum dot lasers," in [*Asia Communications and Photonics Conference and Exhibition*], IEEE (dec 2010).

[3] Otsubo, K., Hatori, N., Ishida, M., Okumura, S., Akiyama, T., Nakata, Y., Ebe, H., Sugawara, M., and Arakawa, Y., "Temperature-insensitive eye-opening under 10-gb/s modulation of 1.3-μm p-doped quantum-dot lasers without current adjustments," *Japanese Journal of Applied Physics* **43**, L1124–L1126 (jul 2004).

[4] Arakawa, Y. and Sakaki, H., "Multidimensional quantum well laser and temperature dependence of its threshold current," *Applied Physics Letters* **40**(11), 939–941 (1982).

[5] Nishi, K., Saito, H., Sugou, S., and Lee, J.-S., "A narrow photoluminescence linewidth of 21 meV at 1.35 μm from strain-reduced InAs quantum dots covered by in0.2ga0.8as grown on GaAs substrates," *Applied Physics Letters* **74**, 1111–1113 (feb 1999).

[6] Hakkarainen, T. V., Schramm, A., Tommila, J., and Guina, M., "The effect of ingaas strain-reducing layer on the optical properties of inas quantum dot chains grown on patterned gaas(100)," *Journal of Applied Physics* **111**, 014306 (jan 2012).

[7] Ustinov, V. M., Maleev, N. A., Zhukov, A. E., Kovsh, A. R., Egorov, A. Y., Lunev, A. V., Volovik, B. V., Krestnikov, I. L., Musikhin, Y. G., Bert, N. A., Kop'ev, P. S., Alferov, Z. I., Ledentsov, N. N., and Bimberg, D., "InAs/InGaAs quantum dot structures on GaAs substrates emitting at 1.3 μm," *Applied Physics Letters* **74**, 2815–2817 (may 1999).

[8] Liu, H. Y., Hopkinson, M., Harrison, C. N., Steer, M. J., Frith, R., Sellers, I. R., Mowbray, D. J., and Skolnick, M. S., "Optimizing the growth of 1.3 μm InAs/InGaAs dots-in-a-well structure," *Journal of Applied Physics* **93**, 2931–2936 (mar 2003).

[9] Lorke, M., Nielsen, T. R., Seebeck, J., Gartner, P., and Jahnke, F., "Influence of carrier-carrier and carrier-phonon correlations on optical absorption and gain in quantum-dot systems," *Physical Review B* **73** (feb 2006).

[10] Bayer, M. and Forchel, A., "Temperature dependence of the exciton homogeneous linewidth In0.60ga0.40as/GaAs-assembled quantum dots," *Physical Review B* **65** (jan 2002).

[11] Matsuda, K., Ikeda, K., Saiki, T., Saito, H., and Nishi, K., "Carrier-carrier interaction in single in0.5ga0.5as quantum dots at room temperature investigated by near-field scanning optical microscope," *Applied Physics Letters* **83**, 2250–2252 (sep 2003).

[12] Borri, P., Langbein, W., Schneider, S., Woggon, U., Sellin, R., Ouyang, D., and Bimberg, D., "Ultralong dephasing time in InGaAs quantum dots," *Physical Review Letters* **87** (sep 2001).

[13] Peyvast, N., Shahid, H., Hogg, R. A., and Childs, D. T. D., "Monte carlo model incorporating many-body effects for determining the gain spectra of quantum dot lasers," *Applied Physics Express* **8**, 122102 (nov 2015).

[14] Yamaguchi, K., Yujobo, K., and Kaizu, T., "Stranski-krastanov growth of InAs quantum dots with narrow size distribution," *Japanese Journal of Applied Physics* **39**, L1245–L1248 (dec 2000).

[15] Sugawara, M., Mukai, K., Nakata, Y., Ishikawa, H., and Sakamoto, A., "Effect of homogeneous broadening of optical gain on lasing spectra in self-assembledInxGa1-xAs/GaAsquantum dot lasers," *Physical Review B* **61**, 7595–7603 (mar 2000).

[16] Grundmann, M. and Bimberg, D., "Theory of random population for quantum dots," *Physical Review B* **55**, 9740–9745 (apr 1997).

[17] Hakki, B. W. and Paoli, T. L., "Gain spectra in gaas doubleheterostructure injection lasers," *Journal of Applied Physics* **46**, 1299–1306 (mar 1975).

[18] Mirin, R. P., Ibbetson, J. P., Nishi, K., Gossard, A. C., and Bowers, J. E., "1.3 μm photoluminescence from InGaAs quantum dots on GaAs," *Applied Physics Letters* **67**, 3795–3797 (dec 1995).

[19] Tisbi, E., Latini, V., Patella, F., Placidi, E., and Arciprete, F., "Anisotropic cation diffusion in the GaAs capping of InAs/GaAs(001) quantum dots," *Journal of Applied Physics* **120**, 235303 (dec 2016).

[20] Garcia, J. M., Medeiros-Ribeiro, G., Schmidt, K., Ngo, T., Feng, J. L., Lorke, A., Kotthaus, J., and Petroff, P. M., "Intermixing and shape changes during the formation of InAs self-assembled quantum dots," *Applied Physics Letters* **71**, 2014–2016 (oct 1997).

[21] Ru, E. C. L., Howe, P., Jones, T. S., and Murray, R., "Strain-engineered InAs/GaAs quantum dots for long-wavelength emission," *Physical Review B* **67** (apr 2003).

[22] Walther, T., Cullis, A. G., Norris, D. J., and Hopkinson, M., "Nature of the stranski-krastanow transition during epitaxy of ingaas on gaas," *Phys. Rev. Lett.* **86**, 2381–2384 (Mar 2001).

[23] Nishi, K., Kageyama, T., Yamaguchi, M., Maeda, Y., Takemasa, K., Yamamoto, T., Sugawara, M., and Arakawa, Y., "Molecular beam epitaxial growths of high-optical-gain InAs quantum dots on GaAs for long-wavelength emission," *Journal of Crystal Growth* **378**, 459–462 (sep 2013).

[24] Vurgaftman, I., Meyer, J. R., and Ram-Mohan, L. R., "Band parameters for III–v compound semiconductors and their alloys," *Journal of Applied Physics* **89**, 5815–5875 (jun 2001).

[25] Peyvast, N., Chen, S., Zhou, K., Babazadeh, N., Khozim, A. A., Zhang, Z., Childs, D. T. D., Wada, O., Hugues, M., Hogg, R. A., Kageyama, T., Nishi, K., Takemasa, K., and Sugawara, M., "Development of broad spectral bandwidth hybrid QW/QD structures from 1000-1400 nm," in [*Novel In-Plane Semiconductor Lasers XIII*], SPIE (feb 2014).

[26] Sobhani, S. A., Childs, D. T., Babazadeh, N., Stevens, B. J., Nishi, K., Sugawara, M., Takemasa, K., and Hogg, R. A., "Study of electro-absorption effects in 1300nm in(ga)as/GaAs quantum dot materials," in [*Physics and Simulation of Optoelectronic Devices XXIV*], SPIE (mar 2016).

[27] Yang, T., Tatebayashi, J., Tsukamoto, S., Nishioka, M., and Arakawa, Y., "Narrow photoluminescence linewidth (<17mev) from highly uniform self-assembled InAs/GaAs quantum dots grown by low-pressure metalorganic chemical vapor deposition," *Applied Physics Letters* **84**, 2817–2819 (apr 2004).

[28] Zhang, Z. Y., Hogg, R. A., Xu, B., Jin, P., and Wang, Z. G., "Realization of extremely broadband quantum-dot superluminescent light-emitting diodes by rapid thermal-annealing process," *Optics Letters* **33**, 1210 (may 2008).